ASTROLABE
A LOW COST AUTONOMOUS STAR CAMERA

Nuno M. GOMES, Marc FOUQUET, Willem H. STEYN

Surrey Satellite Technology Limited

University of Surrey, Guildford, GU2 5XH, United Kingdom

E-mail: N.Gomes@ee.surrey.ac.uk

ABSTRACT - The use of new, low cost, autonomous star sensors is finding its way in an increasing number of small satellites. In this paper, we present some of the characteristics of the new Astrolabe Star Camera together with the processing unit and respective software algorithms developed at SSTL. The research started with the Star Imaging System (SIS), a star sensor test bed, flying since September 1993 in PoSAT-1, a 50 kg microsatellite.

The Astrolabe Star Camera and the computer were built with commercially available off-the-shelf components, excluding only the baffle and casing which were designed in-house. The camera incorporates a wide field-of-view lens, achieving a 99% all-sky availability of 4 stars above the limiting magnitude in the 14.4 by 19.2° FOV.

The software is entirely written in ANSI C code running in a T805 transputer and the algorithms have been validated using in-orbit data from the SIS. An overview of the algorithms will be presented comprising all stages from image to attitude data: image processing, tracking, pattern recognition and attitude calculation. Cosmic radiation induced effects can generate false stars and must not be ignored, as illustrated with image data from the SIS.

The star pattern recognition algorithm allows the star sensor to operate in a fully autonomous mode, making a lost-in-space recovery possible. A subset of the Hipparcos Star Catalogue is used as the operational star catalogue.

1. INTRODUCTION

The importance of autonomous attitude determination has since long been identified in the space industry. Recovery from "lost in space" events and simpler in-orbit spacecraft reasons are some of the reasons why this technology has been pursued over the years. In this context, Surrey Satellite Technology has devoted some of its resources to the development of the Astrolabe Star Camera.

With a very successful remote sensing experience at Surrey, including high-performance on-board data handing, the development programme enhanced the available CCD camera and computing technology to suit the requirements of star attitude determination. The combination of a computer with the use of complex but versatile software, permitted a great degree of flexibility in the camera design, considerably reducing the overall cost of the sensor.

With the lessons learned, in both hardware and software algorithms, with the PoSAT-1 star camera experiment (section 4), the development of the new star camera was initiated in the fourth quarter of 1997. The objective is to demonstrate the operation of a dual camera head star sensing system in the Surrey next generation spacecraft UoSAT-12, a 200 kg minisatellite.
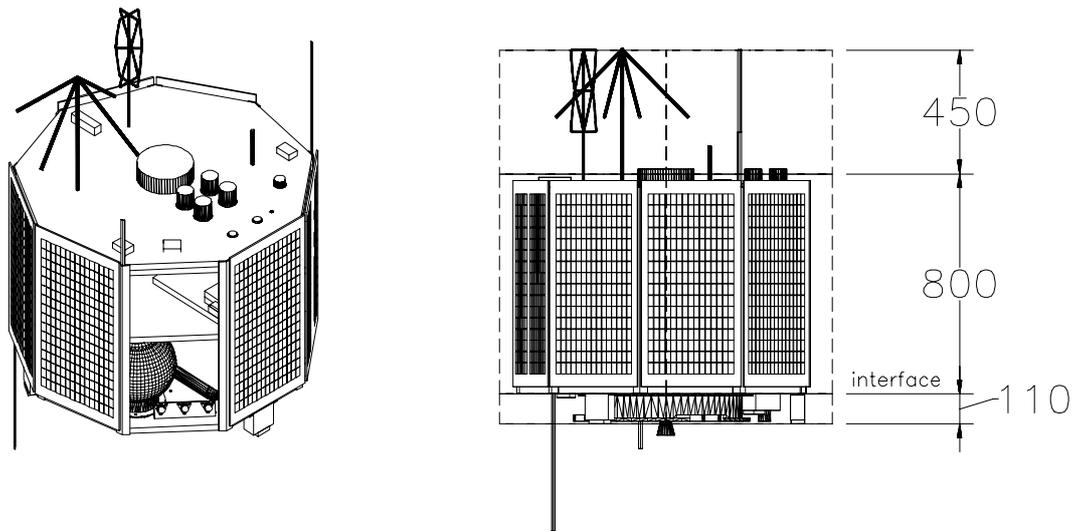

Fig. 1: the minisatellite platform.

The platform is illustrated in Fig. 1. It supports a payload mass from 50 to 150kg and provides it with more than 80W orbit average power. The Orbit Control and Determination System (OCS) comprises a GPS receiver and a cold gas thruster system. Both are also an integral part of the Attitude Control and Determination System (ADCS), which includes two Astrolabe star sensors, magnetometers, magnetorquers, horizon and sun sensors and an offset momentum wheel system.
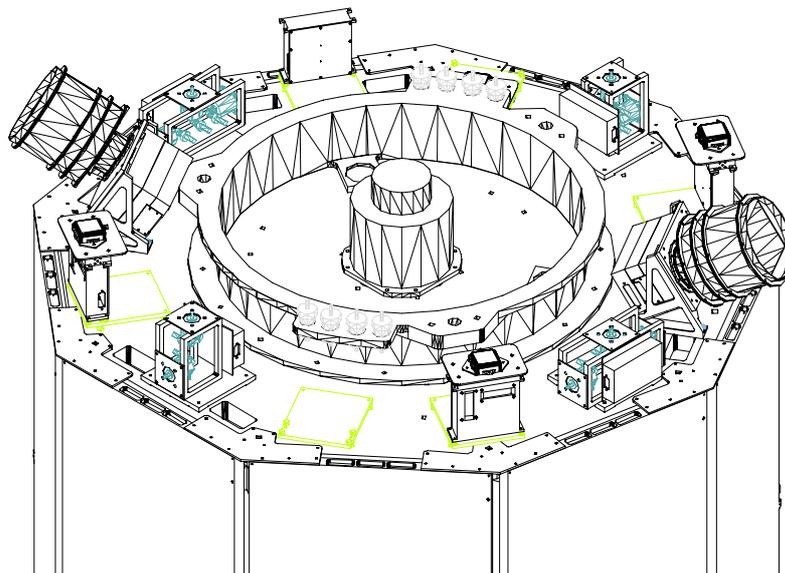

Fig. 2: detail of the space facing facet of UoSAT-12.

The three axis control system maintains Earth pointing to an accuracy of 0.5°, with an experimental target of 0.1°, for Earth observation payloads and communication antennas. The ADCS and OCS are supported by an attitude control processor, which can be any of the four primary on-board processors.

An overview of Astrolabe's camera and computer hardware is given in section 2. The following section describes the software component tasks: image processing, pattern matching and attitude calculation.

2. ASTROLABE

The basic blocks of this type of star sensor are: a **CCD camera** that captures and digitises the star field; a **microcontroller unit** which controls the camera and communications devices; a **processing unit** which executes an elaborate program – effectively making the sensor autonomous – and a **baffle** to shield the active sensor from stray light. Fig. 3 shows the system components.
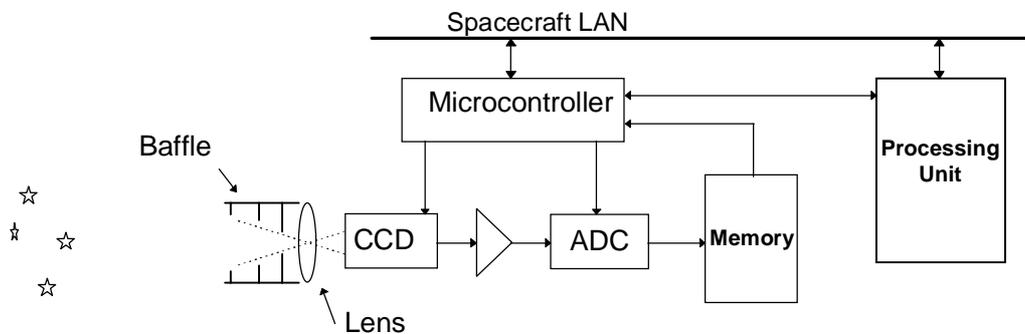

Fig. 3: the Astrolabe Star Sensor components

The sensor is physically divided in two modules, a sensor head comprising the CCD camera and microcontroller and a second module with the processing unit. The modules are connected with a high speed link and through the spacecraft CAN network for telecommand and telemetry. Both modules include electronics to condition the power supplied by the spacecraft bus.

2.1 Sensor head

The sensor head is derived from the fourth generation of UoSAT wide-angle camera series and its role is to capture a digitised image and transfer it to the processing unit. The electronics are distributed on three PCB boards, each enclosed in an aluminium box (Fig. 3), allowing a modular design and minimisation of noise caused by electrical interference.

The first board - the camera – holds the CCD sensor, signal processing and clock generation electronics. The microcontroller, the analogue-to-digital circuitry and image memory are integrated in the middle board. The last board contains the power conditioning electronics (dc-dc convertors and linear devices) used to supply the required voltages from the spacecraft's 28 V non-regulated bus and opto-isolation on all I/O lines.

2.1.1 CCD Camera and optics

The camera design is based on the EEV02-06 scientific CCD sensor, a 2/3" frame transfer device, and associated chipset. Image region B of the CCD is shielded to act as storage, minimising light smear during image readout. The 288 lines by 385 columns image, with a pixel pitch of 22 by 22 μm, is integrated for 200 ms. Anti-blooming is not needed to image stars and it is disabled with the added

advantage of increasing the pixel's well capacity. The 5 IC assembly produces a video signal which, after amplification and filtering, is fed into the microcontroller board for digitisation.

The lens is a commercially available CF25L from Fujinon, Japan, with 25 mm focal length (f) and an aperture of f:0.85. An industry standard C-mount is used to attach the lens to the first box. The combination of these two elements, the CCD and lens, yields a field-of-view (FOV) of 14.5 by 19.2°.
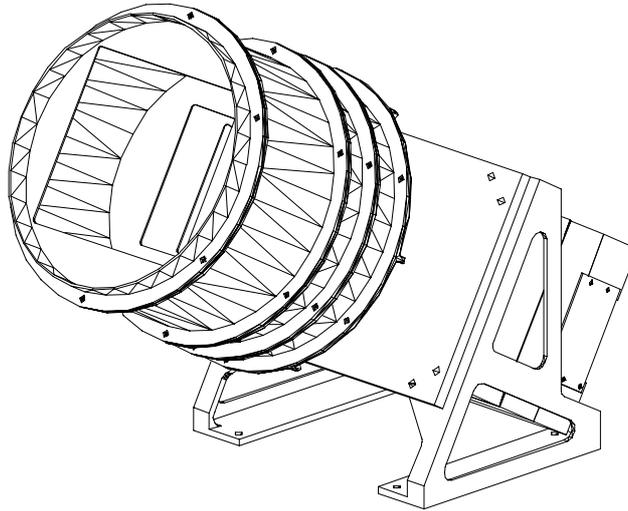

**Fig. 4: astrolabe sensor head with baffle
and attaching structure.**

Using data collected by the experimental star sensor camera in PoSAT-1 (section 4.2), Astrolabe's limiting magnitude can be estimated since the normalised spectral response of both sensors is the same [EEVa 90] [EEVb 90], in other words, both star sensors measure the same relative magnitude or instrumental magnitude (m_I). The calculations yield a value of m_I=5.3 for the limiting magnitude of Astrolabe when the changes in integration time, lens aperture and CCD responsivity are taken into consideration.

The two characteristics, limiting magnitude and FOV, set the sensor's capability to recover from a **lost in space** event. An ideal star sensor would be able to detect the minimum number of stars necessary to determine the spacecraft orientation, with no prior attitude knowledge, anywhere in the celestial sphere – a 100% availability assuming no interference from the Moon, Earth or Sun. But stars are not uniformly distributed and some regions do not have enough bright stars for a successful pattern match.

To determine the expected sensor performance, the input catalogue (section 3.3) was searched in steps of 0.2 degrees in right ascension and declination. For each step, the four brightest stars are selected within a pre-determined FOV size. The faintest of the four gives the limiting magnitude for that particular region and, if compared with the faintest star of all previous steps and found to be even fainter, it is stored for further comparison. After the final step, the magnitude of this star is the limiting magnitude for that FOV size at 100% availability. Other values of availability are determined by finding the limiting magnitude for a given percentage of all the steps. By repeating the procedure for different sizes of FOV, the variation of limiting magnitude requirement with FOV is apparent. The search result is shown in Fig. 5.
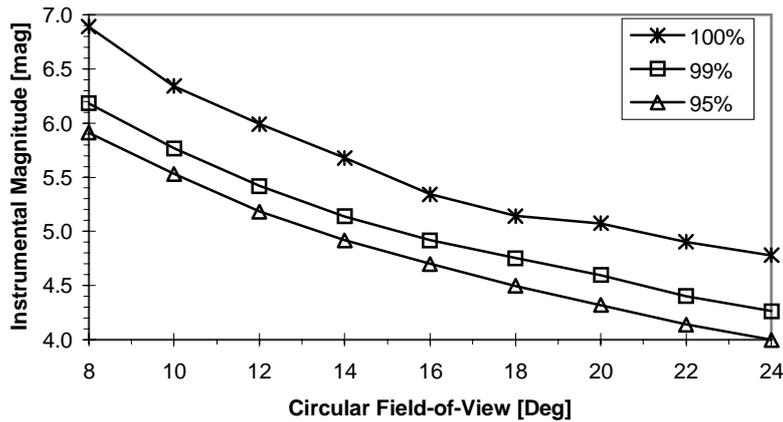
Fig. 5: limiting magnitude needed at various availabilities of a four star pattern.

Astrolabe, with an inscribed circular FOV of 14.5 degrees, must have a limiting magnitude of 5.2 for 99% availability. As stated above, the estimated limiting magnitude is within this requirement. In fact, the margin is larger as the FOV is rectangular and its total angular area is equivalent to a circular FOV of 19.0 degrees. Furthermore, the requirement for a four star pattern is applicable only during initialisation or recovering from a lost in space event, during normal operation the requirement is two stars.

2.1.2 Microcontroller unit

This unit interfaces the sensor head with the rest of the spacecraft and orchestrates the data flow from the CCD to the processing unit through digitisation and storage in image memory. At the heart of the system is a Motorolla 68HC11F1 with 32 kbytes of ROM for program code and 16 kbytes for variables and, if necessary, program updates or patches. The 4 Mbytes of image memory is changed to the first half of the 16 bit address space in a sixty four 32 kbytes pages arrangement. The communications to the outside world are via two mutually redundant CAN interfaces, for telecommand and telemetry, and one 20 Mbit/s high speed INMOS link to the processing unit for imagery download. A multiplexer allows the high speed link to be connected to a spare computer in the event of failure of the primary processing unit.

The analogue video signal is digitised to 8 bits using a SONY CXD1175 two-step flash converter, a low-power chip specifically design for video signals.

Image exposure control is achieved with two methods: integration control and adjusting the reference levels of the ADC chip. Integration control determines how long is the CCD allowed to collected light and can be varied by telecommand between 1 ms to 420 ms, although at integration times higher than 200 ms only one image per second can be collected and are mainly used during camera calibration. The other method works simply by changing the low and high references of the ADC chip, effectively modifying the offset and gain settings of the circuit. This in-orbit flexibility allows the precise tuning of the sensor after launch and during its lifetime, providing some degree of adaptability to changing mission requirements.

2.1.3 Baffle

To minimise stray light in the sensor's FOV, a **diffuse absorbing baffle** was designed with modularity in mind to facilitate the integration in different spacecraft. For the UoSAT-12 satellite, a three vane baffle was chosen as the best compromise between baffle length, sun angle rejection

(SRA), shadowing of solar panels and mechanical integrity during launch. As seen in Fig. 4, the star sensors are tilted (30°) to avoid reflected light from the Earth entering the baffle aperture. This in turn sets the upper limit for the SRA to be 60° so that at least one star sensor is never blinded by the Sun. The maximum length available for the baffle in UoSAT-12 is 11 cm.

The baffle geometry is optimised [Arno 96] to obtain the maximum stray light attenuation possible within the imposed constraints. The internal opening of the vanes, or port, is rectangular and defined by the FOV. The spacing between the vanes – the cavity – follows a set of rules: no direct light from the Sun will illuminate the middle vane for angles larger than the SRA, since the light reflected from this vane to the back first vane (which is visible from lens) is more important than from the cavity walls; the lens aperture – the output port – will not be in direct view of the first cavity walls and the number of illuminated vane edges shall be as small as possible.

The construction of the baffle also obeys simple but effective measures: the vane edge is sharpened, which is specially important in the first vane, and all surfaces are sand blasted and black anodised. The sand blasting is necessary to avoid a "shiny black" effect.

2.2 Processing unit

The star sensor processing unit is an evolved version of the Transputer Module, the imaging computing resource for remote sensing payloads in the UoSAT microsatellite family with a combined in-orbit operational life of 24 years. This module forms part of network of four transputers, T0 to T3, dedicated exclusively to image processing which can also be reconfigured after launch. No loss of operational capability, other than processing power, occurs with a single transputer failure.

The star processing unit, T1, comprises a IMS-T805-G25S transputer [SGST 97] running at an internal clock frequency of 25 MHz. The T805 transputer was specifically designed for parallel processing and features on-chip: 4 kbytes of internal RAM, four high speed INMOS links, 64 bit floating point unit, timers and a programmable external memory interface. Because of the susceptibility of the transputer's internal RAM to radiation effects (both in terms of a poor total dose performance and a vulnerability to single event upsets), these 4 kbytes are permanently disabled in flight, and external RAM is used exclusively.

The transputer chip used for SSTL missions is not procured to any specific military qualification. The decision to use a commercial-spec device is based largely on the vastly increased cost and very limited availability of military-grade transputers. However, all of SGS-Thomson's current devices are manufactured using identical production techniques, and the difference between commercial and military components is the level of post-manufacture screening each device receives before leaving the factory. Therefore, it was not considered a great risk to use a commercial part for the transputer, bearing in mind the testing that it was going to receive during assembly, integration and test of the spacecraft.

The transputer has access to 32 Mbytes of CMOS static RAM arranged as 8 M x 32 made up of 4 M x 8 SIMMs. This memory is divided in two equal parts of Error Detection and Correction (EDAC) protected RAM and non-protected memory. The EDAC protected memory is used to store program code and variables where an error can cause failure of the transputer program. Non-protected memory is only used to store image data which is very short-lived (approximately 1 second) and the SEU probability is therefore very low and of negligible consequence. The absence of EDAC circuitry for the image memory makes it considerably faster than protected memory, a significant time reducing factor during the very intensive image processing.
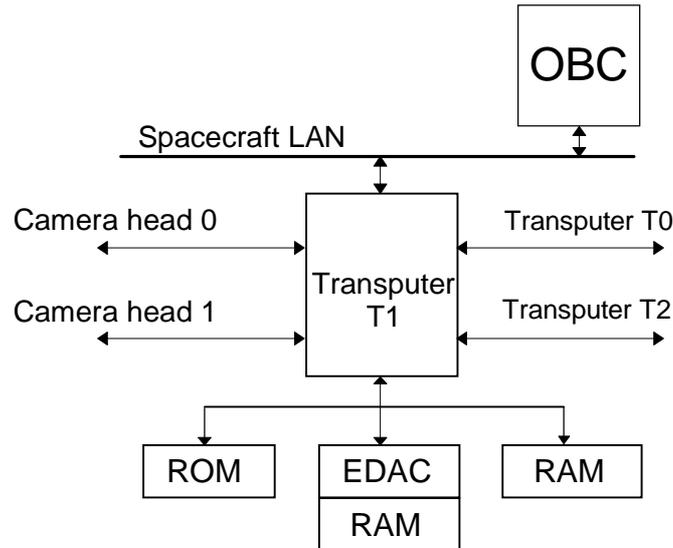
Fig. 6: the processing unit.

The four INMOS links (Fig. 6) are distributed to both star sensor camera heads and two imaging payload transputers. Link 0 and link 1 are connected directly to T0 and T2, respectively. Links 2 and 3 connect the camera heads, each through a multiplexer allowing T2 to replace the processing unit. Two CAN interfaces connect to the dual redundant spacecraft network for telecommand and telemetry. An high-speed Ethernet network (not shown) is used to transmit high volume data (imagery in the case of the transputer) to and from the spacecraft on-board computer or ramdisk.

3. SOFTWARE

The software running in the processing unit has two main functions: to derive attitude data from the imagery and subsystem housekeeping (attitude data dissemination, time keeping and synchronisation, telemetry and telecommand). The discussion below will concentrate on the first part.

The software development started with the experimental star camera flown on PoSAT-1 (section 4). Different strategies for both the image pre-processing or scanning and the identification of the new stars were tested with the imagery available from PoSAT-1.

The basic algorithm is depicted in Fig. 7, upon hardware reset or telecommand the processing unit initialises variables and prepares the star catalogue (section 3.3) into a suitable format for the matching process. Then, the cycle shown is sequentially stepped within the available time: 0.5 s for the UoSAT-12 star sensor.

The software was entirely written in ANSI C and tested successfully on three different types of platforms: SPARC, transputer and PC. No difficulties are foreseen in porting the software to other platforms.

3.1 Tracking and image pre-processing

The image pre-processing detects stars in the sensor FOV and measures their position in the instrument reference frame. The process of detecting stars occurs in stages: candidate pixels are selected, verified and filtered for radiation or noise effects. Each stage should be of increasing complexity since, when processing an image, most of the time is spent selecting the pixels within the constraints for the next stage. The process should take advantage of the fact that a star will normally

illuminate more that one pixel both due to the slightly defocused sensor and light smearing because of the moving spacecraft during the image integration time.
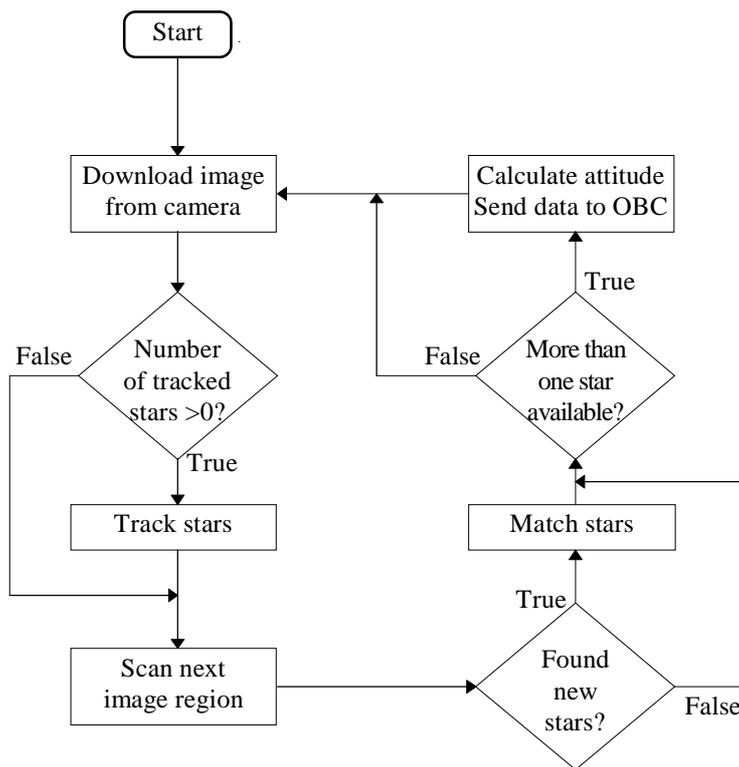

Fig. 7: attitude determination algorithm.

Selecting candidate pixels is normally achieved by setting a threshold and only investigate all pixels above it. Determining the threshold is not trivial, beside the different electrical characteristics of each sensor, the background level of light can vary from image to image and within the same image. The variation is due to the combined effects of stray light entering the lens aperture and the non-uniform distribution of faint objects in the sky. The threshold should be able to cope with changes both in time (image to image) and from within the same image.

The strategy that showed better results is to divide the image in several fractions, slightly overlapping, where the background level can be considered constant. This also adds more flexibility to the overall processing by reducing the image region to be processed in each step, more time can be devoted to other tasks where this division would be difficult to implement, if not counter productive; i.e., the pattern matching task. The threshold is then a function of the image region's statistics. Care must be taken when selecting the size of the regions, as the spurious effects of radiation and under sampling can give rise to wrong threshold estimates. Another side effect is the increased time taken to scan an entire FOV. This time being equal to the total number of regions multiplied by the step period.

If a pixel is found to be above the threshold, it must be brighter than its neighbouring pixels. Otherwise the centre of the star light distribution will be somewhere else. Once this condition is obeyed, a predetermined number of neighbouring pixel must be above a second threshold, smaller than the first. This will eliminate bright single pixel spikes either caused directly by radiation, damaged pixels (hot-pixels) or noise.

The final stage in the process is to remove star-like features caused by radiation in the form of cosmic rays. This can be easily achieved by looking for a similar feature in the previous image within a small search window. If it is caused by cosmic rays, then the feature will be missing from the previous image. Electrical charge collected by the CCD due to radiation effects is short lived.

Once the pixel has been verified as the centre of a star, then the coordinates of that star are measured using a centroiding method. The star's magnitude is determined with aperture photometry where the pixel counts in a predefined window around the star are summed and the estimated sky background is subtracted. The resulting value is the star's total number of counts, sometimes also called grey levels or analogue to digital units (ADUs). This value is converted to instrument magnitude or number of electrons using data from calibration (section 4.2).

To avoid the need for a complete pattern matching for each new image, the software maintains a list of identified stars from the previous image. The stars' position in the new image can be estimated and it is bounded by a window defined by the sensor's maximum angular displacement in the time interval between successive images. The advantages of tracking are significant, since even if only two stars are visible in the FOV, the spacecraft's attitude can still be estimated and the pattern matching algorithm can use this information to dramatically speed up the identification of new stars entering the FOV.

3.2 Pattern matching

The pattern matching is what makes the star sensor autonomous. It enables the determination of attitude, needing only the data supplied by the image pre-processing (star position in the instrument frame and measured magnitude) and/or by the tracking (star position in instrument and inertial reference frame and measured magnitude). No interaction with other spacecraft subsystems is necessary. Pattern matching is only performed if one or more new stars enters the FOV, during initialisation or by telecommand from the onboard computer or control groundstation.
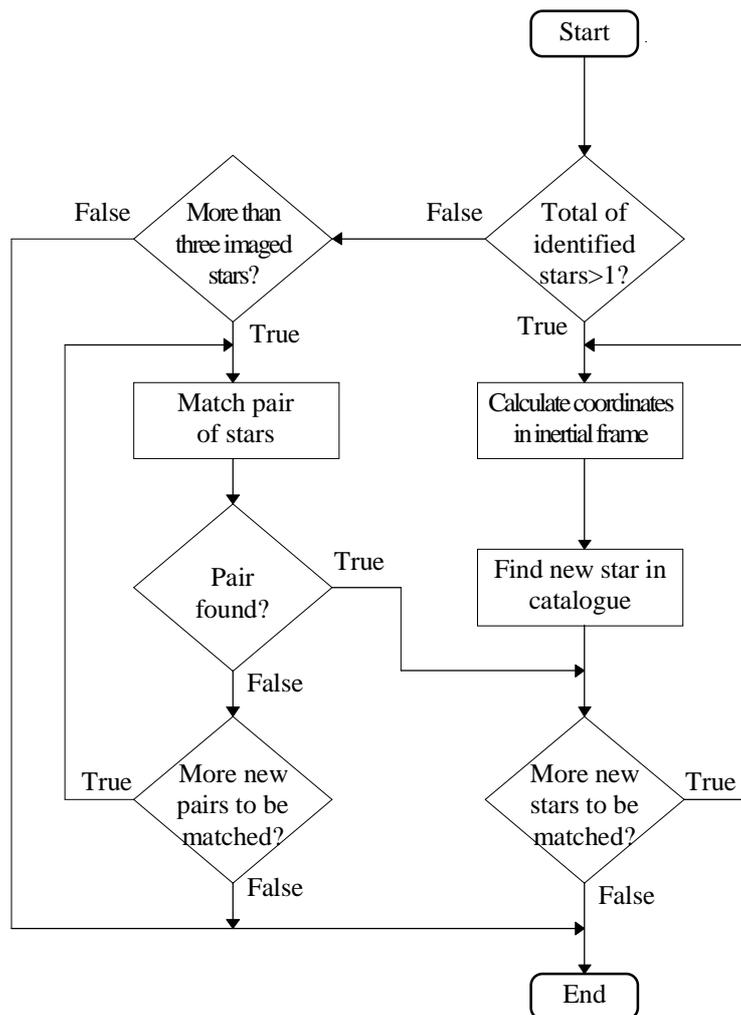

Fig. 8: pattern matching algorithm.

The task is divided in two parts so as to use all the available information in the most efficient way possible, depending on the number of tracked stars previously identified. If two or more identified stars have been successfully tracked, then the position of the new star(s) in the inertial reference coordinate system can easily be estimated using any of the methods described in section 3.4. A very small portion of the star catalogue is then searched for a matching star in both position and magnitude.

If less than two identified stars are tracked but the total number of observed stars is above three, a search of the entire catalogue is made. The only available information invariant to rotation and translation of the FOV in the celestial sphere is the angular distance and star magnitude. The method found to be the most suitable is a variation of the **polygon angular separation match** technique [Wert 85] for patterns of three or more stars.

A pattern of stars is considered to be matched to a corresponding pattern in the catalogue if the following conditions are met:

- All combinations of observed angular distances must be within a given tolerance (ε) with the corresponding angular distance in the catalogue;

- Each measured star magnitude must be within a given tolerance (τ) to the corresponding star in the catalogue;

- The pattern in the catalogue must not be the mirror image of the observed pattern.

Although theoretically a minimum of three stars is required to apply this technique, in practice the probability of a wrong match for a three star pattern is too high and at least four must be used. If more than four stars are available for matching, the algorithm is immune to a limited number of false stars and it will step through all the possible combinations of four stars until the above conditions are met. Nothing is gained by scanning all combinations, since even if a pattern is matched with less total error (distance and magnitude), it does not signify the match to be more correct.
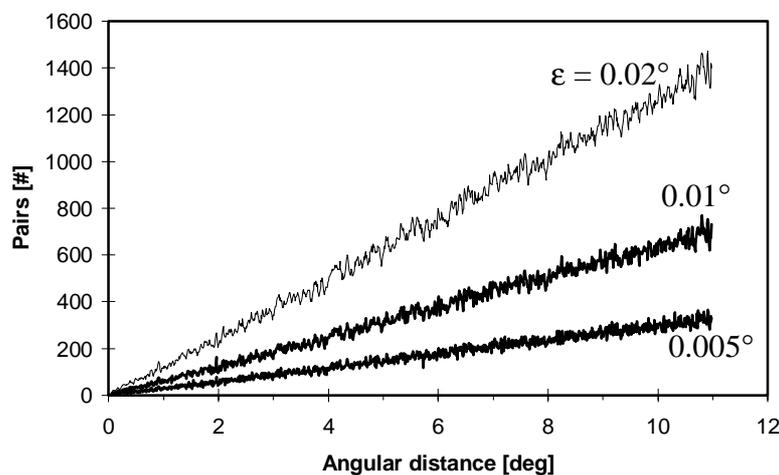

Fig. 9: number of matching pairs in the catalogue with varying distance and for a given tolerance (ε).

Searching the catalogue with only distance and magnitude information is time consuming. However, by careful selection of the stars and matching method, the search time can be optimised. Firstly, it can be seen that only the first pair needs to be searched by angular distance, all the others can be found by estimating their position and searching the catalogue in a similar way to the first matching

method described above. In order to further speed up the initial search, the first pair of pairs should have the smallest distance. The reason to this can be explain from Fig. 9.

The graph above shows the number of pairs within a given tolerance and angular distance. The data was retrieved from the PoSAT-1 catalogue with 6431 stars. The number of matching pairs varies almost linearly with distance and tolerance. A result of this analysis is the trade-off in processing time between sensor accuracy and computer power.

3.3 Star catalogue

The input star catalogue is a subset of the Hipparcos Catalogue [ESA 97] based on observations made with the ESA Hipparcos astrometry satellite. The information is given for epoch J1991.25 in the ICRS (International Celestial Reference System) consistent with the J2000 (FK5) reference system. Analysis of the magnitude distribution of its 118128 entries indicates that the catalogue is comprehensive to instrument magnitude (m_H) brighter than 7.5 [Mign 97]. The catalogue is accurate to less than one milliarcsec (mas) for stars brighter than $m_H = 9$ at the catalogue epoch (J1991.25) and less than 2.3 mas at J2000.0 (< 0.25 mas/yr) [Perr 97]. Besides the positional data, Astrolabe's input catalogue makes use of photometric data (V magnitude and B-V colour parameter in the Johnson UBV photometric system), proper motion and star magnitude variability.

Stars were selected in several stages. The instrument magnitude (m_I) was calculated for each entry using calibration data from PoSAT-1 and stars are merged into one if separated by less than the field of view one pixel. Stars fainter than $m_I = 6$ and flagged with a magnitude variability of 0.1 or more were rejected. To remove the excess stars in certain sky regions, a full sky search in steps of 0.2 deg in both right ascension and declination was performed. Only the five brightest stars in a suitable circular FOV size were selected. Approximately 3000 stars were finally selected (Fig. 10).
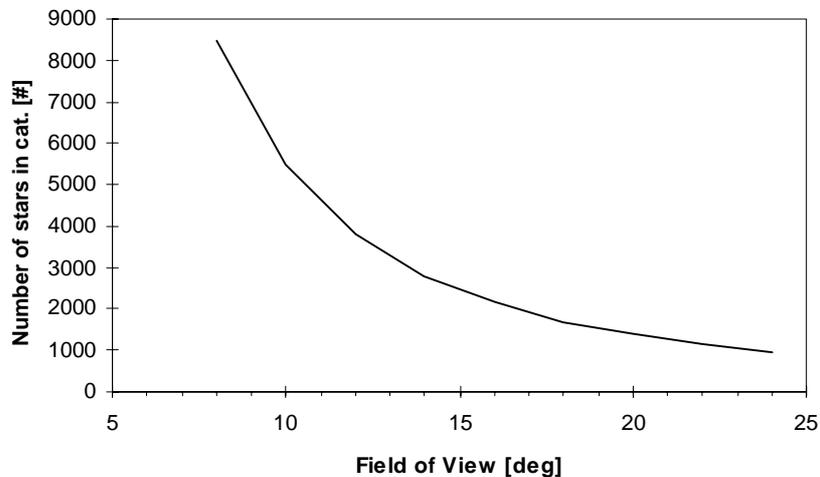

**Fig. 10: number of stars in final
catalogue with varying FOV size.**

The final list of stars is then corrected for the mission mean epoch and choice of inertial reference system. The star's position is propagated to 2002 (launch is expected in April 1999). The calculations for the rigorous epoch transformations is found in volume 1 of [ESA 97].

3.4 Attitude calculations

To determine the three-axis attitude of a satellite from vector observations, two methods [Wert 85] are available depending on the number of available measurements: the algebraic method or TRIAD

and the q-method. Both methods are used depending on the number of available vector measurements.

TRIAD is deterministic and therefore fast, but only applicable for two vector measurements. The q-method is an algorithm that optimally determines the attitude (the quaternion) using n measurements, although at a considerable increase in computational processing as a eigenvalue equation must be solved usually by numeric methods. An approximation scheme to the q-method, QUEST or quaternion estimation [Shus 81], permits the fast computation of the optimal quaternion to an arbitrarily high accuracy without the eigenvalue equation.

The output of TRIAD is an attitude transformation matrix (a rotation matrix from the inertial reference system to the instrument reference) and QUEST delivers the optimal quaternion. The attitude data can be converted to the most suitable format.

To simplify the interaction between the star sensor and the rest of the spacecraft, the software does not keep track of the satellite's position. As such, the aberration effects are not compensated in the attitude solution. This can lead to an error of less than 25 arcsec. If higher accuracy is desirable, the sensor can provide the vector measurements directly to the OBC.

4. POSAT-1

The PoSAT-1 satellite was Portugal's first spacecraft, jointly built by a consortium of Portuguese companies and Surrey Satellite Technology Ltd. (SSTL) at the University of Surrey as part of a Technology Transfer programme. Launched into orbit on September 26th 1993, aboard an Arianne IV launcher from Kourou, French Guiana. The spacecraft is a UoSAT type of microsatellite (Fig. 11) with a mass of 50 kg, based on a design developed by SSTL with the experience of seven previous missions.
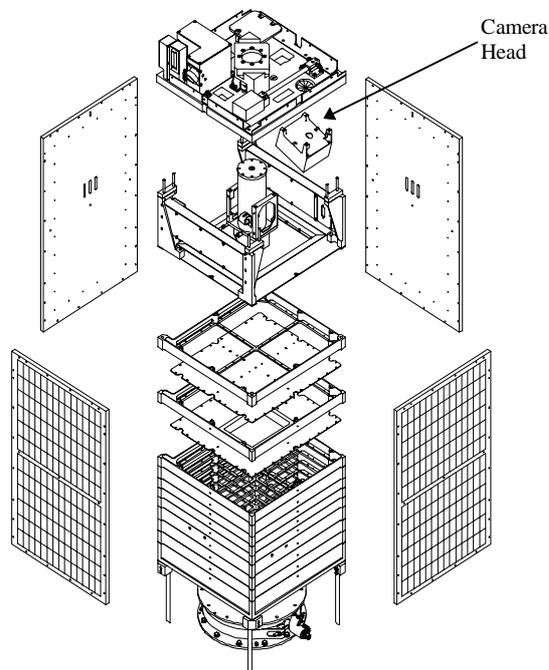

Fig. 11: exploded view of PoSAT-1 in launch configuration.

The satellite, which is in a sun-synchronous orbit at an altitude of 800 km with 98.6° of inclination, has a modular architecture similar to UoSAT-5 launched in 1991 and carries several experiments on-board:

- The Earth Imaging System (EIS) consists of two monochromatic CCD cameras, with a ground resolution of approximately 2 km and 200 m.

- The Cosmic Ray Experiment (CRE) and Total Dose Experiment (TDE) monitors the radiation environment in PoSAT-1's orbit.

- An experimental Global Positioning System receiver providing a unique capability (at the time of launch) of precise orbit determination and automatic on-board generation of keplerian elements.

- A communications payload, implementing SSTL's store and forward protocols, used extensively by a range of users, including the Portuguese military.

- The Star Imaging Sensor (SIS) experiment based on the EIS camera design, optimised for star imaging. The experiment is described in more detail below.

After almost five years in orbit, all the spacecraft's subsystems are fully functional. The advanced On-Board Computer system allows a near autonomous operation with only one person at the Control Ground Station providing all the necessary supervision. The Ground Station is situated in Sintra, Portugal, at the satellite communications site of Marconi, one of the consortium companies.

4.1 Star Imaging System

In PoSAT-1, the SIS is not integrated in one single box but it is physically divided in two sections: a camera head, holding all the CCD electronics and the lens, is located below the spacecraft's top facet (Fig. 11); the analogue-to-digital-conversion, buffers and microcontroller are integrated in one electronic board in the same tray as the GPS receiver.

The active sensor is a CCD04-06 from EEV Ltd, U. K. [EEVb 91]. The CCD has a 288 by 576 matrix of rectangular pixels (22.5 by 15.0 µm) digitised to 8 bit. The lens is a 50 mm focal length Cosmicar with an aperture of f/1.4. The resulting FOV is 7.3 by 9.7 degrees and the instantaneous field of view (IFOV) is 0.017 by 0.026 degrees. The microcontroller is a 68HC11 from Motorolla.

The Processing Unit comprises two T805 transputers, T0 and T1, running at a clock frequency of 20 MHz. The primary processor, T1, has 2Mbytes of EDAC protected memory. Transputer T0 acts as a backup of T1 and having 1 Mbyte of unprotected memory. The processors are shared with the EIS and GPS subsystems.

Following T1's command, the SIS captures a set of up to 4 images. The images are separated by 542 ms and the integration time can be set from 20 to 136 ms. The images are downloaded to the transputer for processing and storage over a 10 Mbit/s link. However, the microcontroller's slow handling of data prevents a transfer time of less than 30 s for a complete set. After processing the images are stored in the spacecraft's ramdisk, transferred across the local network.

The absence of a baffle and the long transfer time limits the usefulness of the SIS as an operational attitude sensor. As a result, the processing is limited to a high-ratio (80:1) image compression for subsequent image manipulation in the ground.

4.2 Results

PoSAT-1 SIS has proved to be a valuable research platform to test calibration methods in orbit and to validate the algorithm implemented in the processing of star sensor imagery in order to obtain attitude data.

The SIS has captured several thousand compressed and uncompressed images. Fig. 12 shows 3250 individual stars in the inertial coordinate system (right ascension and declination). Some of these stars where repeatedly imaged (on average 18 times per star). The image data was captured between January 1994 and April 1998.
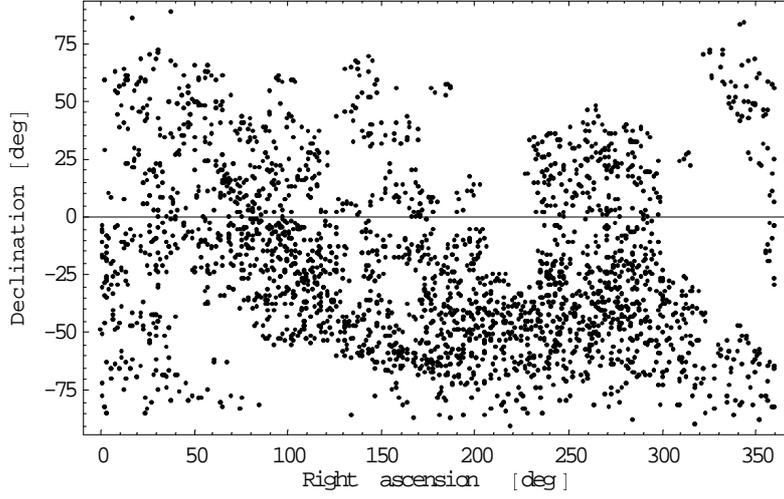
Fig. 12: imaged stars (J2000 coordinate system).

Using the photometric data supplied by the input catalogue (section 3.3) and the measured star brightness in ADU (analogue to digital units or grey levels), the sensor's colour correction function $m_I - m_V = (I-V)$ was determined forming a fourth-order polynomial fit:

$$(I - V) = R(B - V) = a_0 + a_1(B - V) + a_2(B - V)^2 + a_3(B - V)^3 + a_4(B - V)^4 \qquad (4.1)$$

Using the usual definition of star magnitude: $R(0) = 0 : a_0 = 0$. Assuming that the relation between measured ADU and star brightness is linear:

$$m_I = I = -2.5 \text{Log}_{10}(C_0 \times \text{adu}) - C_1 \qquad (4.2)$$

Where C_0 is the gain, given in [erg cm^{-2} s^{-1} ADU^{-1}], and C_1 is the zero magnitude (instrument) type A0-V as defined in the Johnson photometric system. Combining the two equations:

$$-2.5 \text{Log}_{10}(C_0 \times \text{adu}) - C_1 - V = a_1(B - V) + a_1(B - V)^2 + a_1(B - V)^3 + a_1(B - V)^4 \qquad (4.3)$$

or

$$-2.5 \text{Log}_{10}(\text{adu}) - V = b_0 + b_1(B - V) + b_1(B - V)^2 + b_1(B - V)^3 + b_1(B - V)^4 \qquad (4.4)$$

where $b_0 = 2.5 \text{Log}_{10}(C_0) + C_1$ and $b_x = a_x, x = \{1,2,3,4\}$.

The solution of eq. 4.4 is trivial. The right side is known from the measurements and the catalogue and left side is simply a fourth-order polynomial in B-V. The numerical solution is shown in Fig. 13.
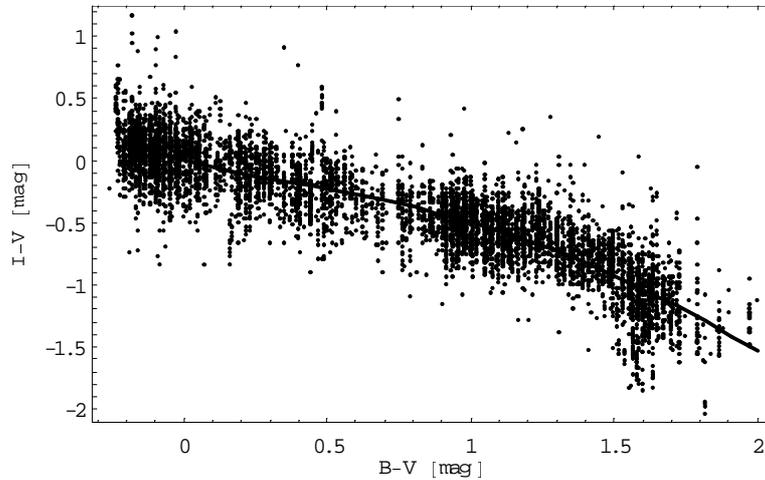

Fig. 13 - Colour correction.

To determine the limiting magnitude, the catalogue was searched for stars within all the imaged sky areas with successful star pattern matches. The search is shown as an histogram of imaged and catalogue stars in Fig. 14. The limiting magnitude is defined as the magnitude of a star for which there is a 50 percent probability of being imaged. By dividing the number of imaged stars by the number of catalogue stars, this probability as a function of star instrument magnitude can be estimated. In Fig. 15 the limiting magnitude of PoSAT-1's SIS can be seen to be 5.1 (approximately).
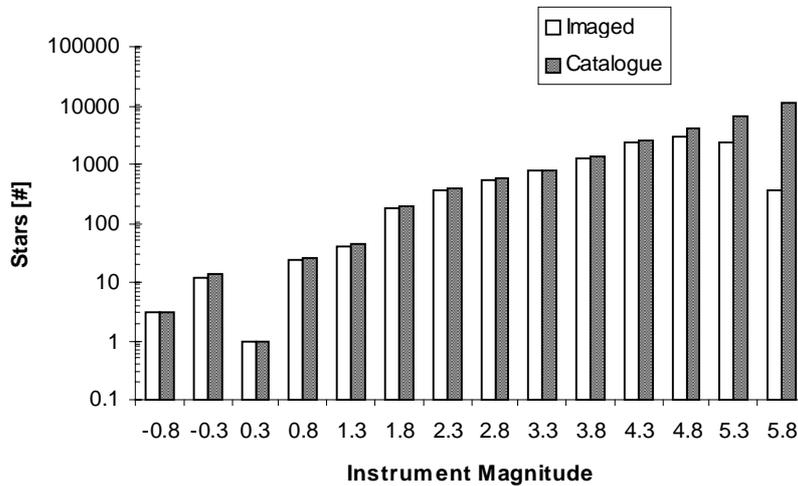

**Fig. 14 - Histogram of instrument star magnitude
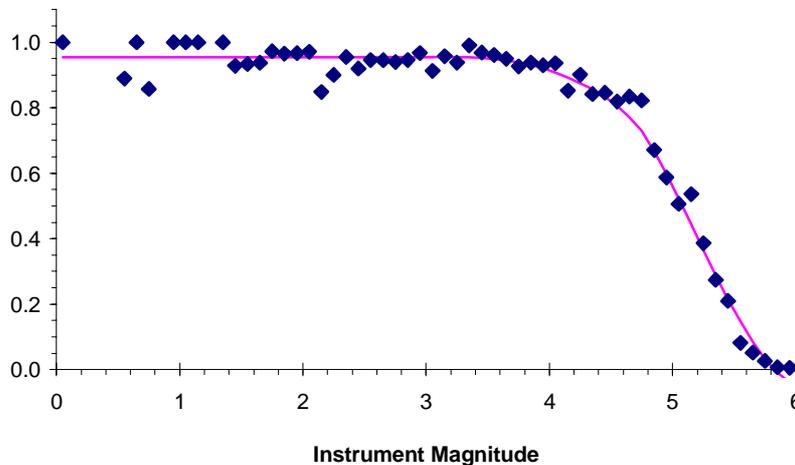in the catalogue and imaged.**

Fig. 15 - Limiting magnitude.

The sensor star position accuracy can be estimated from the difference in angular distance between imaged star pairs and the corresponding star pair angular distance in the catalogue (assumed to be noiseless). The histogram of these differences is shown in Fig. 16. The standard deviation of the differences is $\sigma_{dif} = 24.6$ arcsec. The standard deviation of star position is then 16.7 arcsec. The value of ε, the tolerance in the matching process, is normally three times this value.

A similar approach can be applied to estimate the sensor magnitude accuracy and the model described above. Fig. 17 shows the histogram of the differences in instrument magnitude of 6372 matched stars. The standard deviation is 0.19 mag.
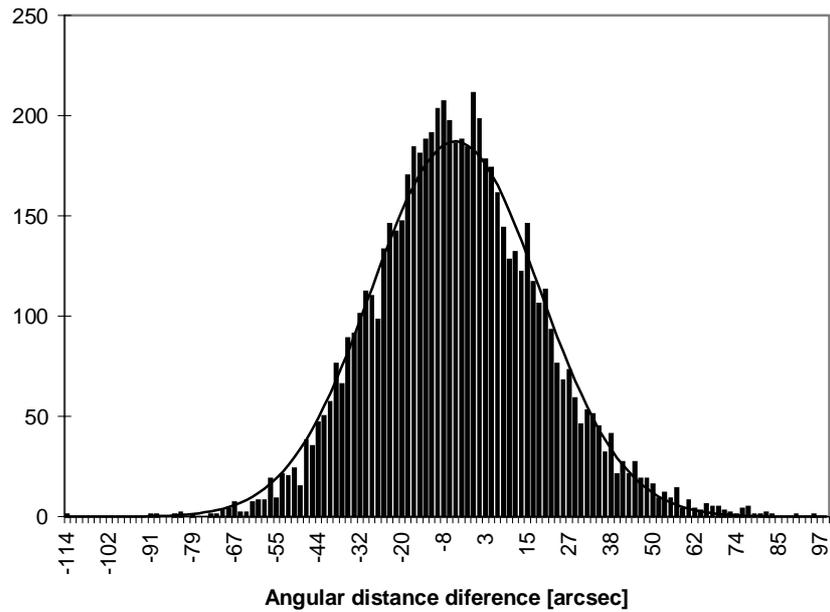
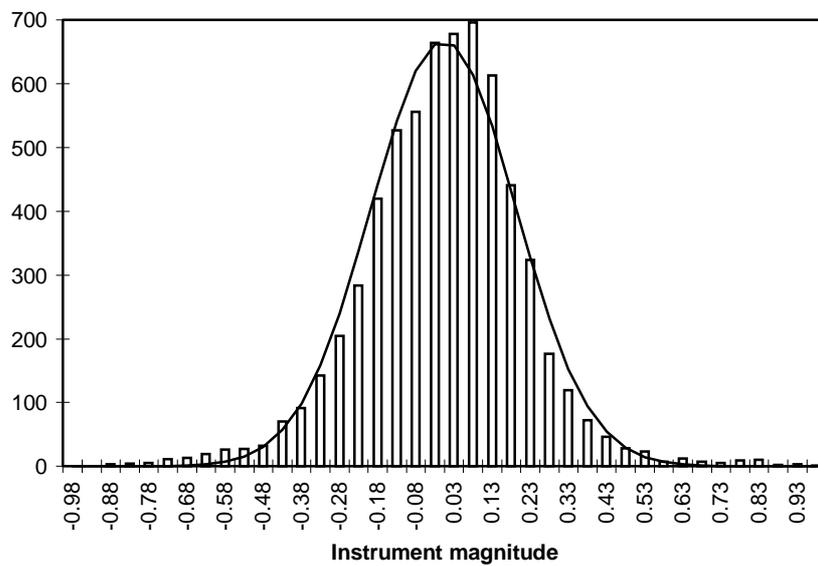**Fig. 16 - Histogram of the differences in angular distance.**

Fig. 17 - Histogram of the differences in star magnitude.

5. CONCLUSIONS

Surrey Satellite Technology has successfully developed a low-cost star attitude determination sensor, the Astrolabe Star Sensor. The reuse of in-house expertise and technology allowed the development concurrently with other programmes (remote sensing CCD cameras and on-board data handling), maximising the available resources and reducing development costs.

The results of PoSAT-1 star camera experiment presented here permitted the construction of software algorithms to achieve an autonomous star sensor with a degree of immunity from transient radiation effects and added experience of in-orbit star camera testing.

The minisatellite UoSAT-12 will allow a definite in-orbit confirmation of high-availability of Astrolabe attitude data to the on-board computer and other subsystems. This will result in all other attitude sensors (including the expensive horizon sensor) to become redundant, simplifying mission design and significantly reduce the cost of small satellites.

6. ACKNOWLEDGEMENTS

7. REFERENCES

[Arno 96]   J. J. Arnoux: "Star sensor baffle optimization", *Optical System Contamination V, Stray, Light and System Optimization*, Proc. SPIE, vol. 2864, November 1996, pp. 333-338.

[EEVa 90]   "CCD02-06 Series Scientific Sensor", EEV Limited, Chelmsford, United Kingdom, Issue 1, A1A-44, June 1990, pp. 1 - 8.

[EEVb 90]   "CCD04-06 TV Image Sensor", EEV Limited, Chelmsford, United Kingdom, Issue 1, A1A-44, June 1990, pp. 1 - 8.

[ESA 97]   ESA: "The Hipparcos and Tycho Catalogues", ESA SP-1200, 1997.

[Mign 97]   F. Mignard: "Astrometric proprieties of the Hipparcos Catalogue", *Proc. from the Hipparcos Venice '97 symposium*, Venice, Italy, May 1997, pp. 5- 10.

[Perr 97]   M. A. C. Perryman et al.: "The Hipparcos Catalogue", *Astronomy and Astrophysics Letters*, vol. 323, July 1997, pp. L49-L52.

[Shus 81]   M. D. Shuster, S. D. Oh: "Three-Axis Attitude Determination from Vector Observations", *Journal of Guidance and Control*, vol. 4, no. 1, February 1981, pp. 70 - 77.

[SGST 97]   "IMS T805 - 32 bit floating point transputer", datasheet, SGS Thomson Microelectronics, February 1997.

[Wert 85]   J. R. Wertz (ed.): "Spacecraft Attitude Determination and Control", D. Reidel Publishing Company, Dordrecht, The Netherlands, 1985.